Current Biology 23, 523–528, March 18, 2013 ©2013 Elsevier Ltd. http://dx.doi.org/10.1016/j.cub.2013.02.018

Report

Evolution of *mir-92a* Underlies Natural Morphological Variation in *Drosophila melanogaster*

Saad Arif,[1,2,7] Sophie Murat,[1,2,7] Isabel Almudi,[1] Maria D.S. Nunes,[1] Diane Bortolamiol-Becet,[6] Naomi S. McGregor,[1] James M.S. Currie,[1] Harri Hughes,[1] Matthew Ronshaugen,[3] Élio Sucena,[4,5] Eric C. Lai,[6] Christian Schlötterer,[2] and Alistair P. McGregor[1,2,*]

[1]Department of Biological and Medical Sciences, Oxford Brookes University, Gipsy Lane, Oxford OX3 0BP, UK

[2]Institut für Populationsgenetik, Veterinärmedizinische Universität Wien, Veterinärplatz 1, 1210 Vienna, Austria

[3]Faculty of Life Sciences, University of Manchester, Oxford Road, Manchester M13 9PT, UK

[4]Instituto Gulbenkian de Ciência, Apartado 14, 2781-901 Oeiras, Portugal

[5]Departamento de Biologia Animal, Faculdade de Ciências, Universidade de Lisboa, Campo Grande, 1749-016 Lisboa, Portugal

[6]Sloan-Kettering Institute, 1017C Rockefeller Research Labs, 1275 York Avenue, Box 252, New York, NY 10065, USA

Summary

Identifying the genetic mechanisms underlying phenotypic change is essential to understanding how gene regulatory networks and ultimately the genotype-to-phenotype map evolve. It is recognized that microRNAs (miRNAs) have the potential to facilitate evolutionary change [1–3]; however, there are no known examples of natural morphological variation caused by evolutionary changes in miRNA expression. Therefore, the contribution of miRNAs to evolutionary change remains unknown [1, 4]. *Drosophila melanogaster* subgroup species display a portion of trichome-free cuticle on the femur of the second leg called the "naked valley." It was previously shown that *Ultrabithorax* (*Ubx*) is involved in naked valley variation between *D. melanogaster* and *D. simulans* [5, 6]. However, naked valley size also varies among populations of *D. melanogaster*, ranging from 1,000 up to 30,000 μm^2. We investigated the genetic basis of intraspecific differences in the naked valley in *D. melanogaster* and found that neither *Ubx* nor *shavenbaby* (*svb*) [7, 8] contributes to this morphological difference. Instead, we show that changes in *mir-92a* expression underlie the evolution of naked valley size in *D. melanogaster* through repression of *shavenoid* (*sha*) [9]. Therefore, our results reveal a novel mechanism for morphological evolution and suggest that modulation of the expression of miRNAs potentially plays a prominent role in generating organismal diversity.

Results and Discussion

Intraspecific Variation in the Naked Valley

The naked valley exhibits considerable intraspecific variation in *D. melanogaster*, ranging from a trichome-free patch as small as 1,000 μm^2 to a naked region of up to approximately 30,000 μm^2 (Figure 1; see also Figure S1 available online). Moreover, small and large naked valley phenotypes segregate within natural *D. melanogaster* populations (Figures 1 and S1). In contrast, among *D. simulans* (Figure S1), *D. mauritiana*, and *D. sechellia* populations, as well as *D. yakuba*, we have only observed naked valley areas at the higher end of the size range (13,000 to 30,000 μm^2). Therefore, small naked valleys (SNVs) appear to be a derived morphological feature within *D. melanogaster*, whereas larger naked valleys (LNVs) are likely to be ancestral with respect to the *D. melanogaster* species subgroup.

Mapping the Genetic Basis of Naked Valley Variation in *D. melanogaster*

It was previously shown that the Hox gene *Ultrabithorax* (*Ubx*) contributes to the difference in naked valley size between a *D. melanogaster* strain with a small naked valley and *D. simulans* [6]. Therefore, to determine whether *Ubx* is also responsible for intraspecific naked valley variation in *D. melanogaster*, we performed quantitative trait locus (QTL) mapping of naked valley size on chromosome 3 among backcross progeny from crosses between strains *st, ss, e* (LNV) and Oregon-R (SNV). We found a single QTL at 88.2 cM on chromosome 3 that explains up to 91% of the difference in naked valley size between the two parental strains (Figure S2A; Table S1), and, using a male F1 backcrossing strategy, we determined that the remaining effect (approximately 10%) is caused by chromosome 2 ($p < 0.017$, Bonferroni corrected pairwise comparison of means). Chromosomes X and 4 have no significant effect. Our mapping thus excludes both *Ubx*, which is at 58.8 cM on chromosome 3 (Figure 2), and the X-linked gene *shavenbaby* (*svb*), which is known to underlie variation in larval trichome patterns [10–12].

To verify that variation in *Ubx* is not responsible for differences in the naked valley in *D. melanogaster*, we carried out two further experiments. First, we repeated our chromosome 3 mapping strategy with two different *D. melanogaster* strains, RAL514 and *ebony* (*e*), *white ocelli* (*wo*), *rough* (*ro*), which have SNVs and LNVs, respectively. QTL mapping using these three recessive markers confirmed the position of a single, large-effect QTL on chromosome 3 at 79.7 to 89.7 cM (2 LOD interval), between *wo* and *ro* (Figure S2A; Table S1). Second, we generated flies with recombinant third chromosomes: homozygous for the *Ubx* allele from a LNV background (Ubx^L) and homozygous for the QTL region from a SNV background (QTL^S), and vice versa (Ubx^S and QTL^L) (Figure S2B). The size of the naked valley of these flies was determined by the background from which the QTL region originated (Figure S2), and no significant effect could be attributed to *Ubx*: flies homozygous for Ubx^L and QTL^S had a small naked valley, whereas flies homozygous for Ubx^S and QTL^L had a large naked valley. Furthermore, the effect on naked valley area of homozygosity for QTL^L or QTL^S was consistent with the QTL mapping results (Figure S2). Our mapping results therefore showed that neither *Ubx* nor *svb* contributes to naked valley variation in *D. melanogaster*.

To fine map the causative locus or loci in the QTL region, we took advantage of the large effect of the QTL and employed the

[7]These authors contributed equally to this work

*Correspondence: amcgregor@brookes.ac.uk

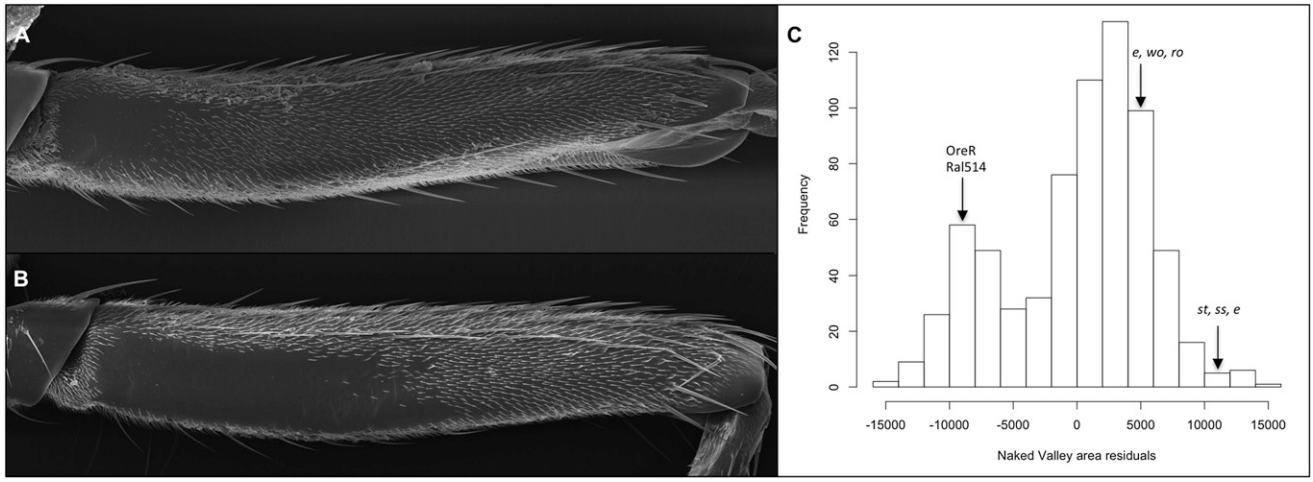

Figure 1. Distribution of Naked Valley Sizes across *D. melanogaster* Populations

(A and B) Posterior femurs of the second legs of *D. melanogaster* strains Oregon-R (A) and *e, wo, ro* (B). Proximal is to the left and distal to the right in both panels.

(C) Bimodal frequency distribution of naked valley phenotypes (residuals of naked valley area regressed on femur length) of 679 male flies from isofemale lines of five populations sampled from Kenya, Turkey, Spain, and the USA. A minimum of three individuals were sampled for each isofemale line. Average values for strains Oregon-R, RAL514, *e, wo, ro*, and *st, ss, e* are indicated by arrows.

See also Figure S1.

visible flanking markers *wo* and *ro* to screen for recombinants. We measured the naked valley area of these flies and scored them for microsatellite, nucleotide, and restriction fragment length polymorphism markers (Figures 2 and S2C). This strategy allowed us to map the causative locus to a region of 25 kb that contains only four genes: part of *Npl4 ortholog*, *Succinic semialdehyde dehydrogenase* (*Ssadh*), *jing interacting gene regulatory 1* (*jigr1*), and *mir-92a* (Figures 2 and S2C). *Npl4 ortholog* is thought to be the homolog of the yeast nuclear pore protein [13]. *Ssadh* encodes a ubiquitously expressed metabolic enzyme [14], and *jigr1* has been implicated in axonal guidance [15]. None of these protein-coding genes is known to be involved in trichome development. However, genome-wide analysis has shown that miR-92a and its seed relatives have the unique ability to induce trichome loss when ectopically expressed during wing development [9, 16] (Figure S3). Therefore, *mir-92a* represented a strong candidate for the evolution of the naked valley.

Functional Analysis of *mir-92a* in Naked Valley Development

To investigate the role of miR-92a in naked valley development, we overexpressed *UAS-mir-92a* [16] using a *heat-shock-GAL4* driver in pupal legs between 8 and 24 hr after puparium formation (APF), when the naked valley pattern is determined [6]. Whereas control flies displayed comparatively small naked valleys, overexpressing *mir-92a* by applying heat shock at 8, 16, or 24 hr APF resulted in flies with progressive loss of trichomes and therefore larger naked valleys (Figure 3). Indeed, the posterior T2 femurs of flies heat shocked at 24 hr APF displayed only a few trichomes (Figure 3D). Driving *UAS-mir-92a* with *dac-GAL4* (which is expressed in the developing femur [17]) also resulted in loss of trichomes and an enlarged naked valley with respect to controls (Figures 3E and 3F). These experiments show that *mir-92a* can repress trichomes on the femur and that variation in *mir-92a* expression modulates the size of the naked valley.

Comparison of the sequences of *mir-92a* between *D. melanogaster* strains with large and small naked valleys shows that the 22 nt sequence that constitutes the mature miRNA and the flanking 200 bp immediately upstream and downstream are identical in both strains (Figure S4A). This suggests that differences in one or more *cis*-regulatory regions (for example, enhancer sequences or splice sites) of *mir-92a*, rather than changes to the primary structure of this miRNA or differential arm usage, are responsible for naked valley evolution. To test this hypothesis, we carried out in situ hybridization against the primary miRNA transcripts to assess expression of *mir-92a* at 24 hr APF in the legs of *D. melanogaster* strains with LNVs and SNVs (*e, wo, ro* and Oregon-R). We found that *pri-mir-92a* expression in the posterior T2 femurs is expanded in *e, wo, ro* compared to Oregon-R (Figure 4D and 4E). This finding is consistent with the difference in the size of the naked valleys between these strains and therefore supports the notion that changes in the regulation of *mir-92a* expression underlie intraspecific variation in the naked valley.

It was previously shown that *Ubx* is involved in trichome development and the evolution of the naked valley between species, although the precise causative changes in *Ubx* have not yet been identified [5, 6]. The involvement of *Ubx* in interspecific differences was demonstrated in part via interspecific complementation tests, where flies carrying a single functional copy of *Ubx* from *D. simulans* had a larger naked valley that those with a single functional copy of *Ubx* from *D. melanogaster* in an otherwise identical genetic background [6]. However, these experiments also showed that flies with *D. melanogaster* chromosomes had consistently smaller naked valleys than those with *D. simulans* chromosomes irrespective of whether the *D. melanogaster* chromosome carried a nonfunctional *Ubx*, which Stern concluded was caused by the involvement of at least one other gene [6]. Because Stern's findings can be interpreted as showing that flies with *mir-92a* from *D. melanogaster* have smaller naked valleys than those with this factor from *D. simulans*, it is possible that the

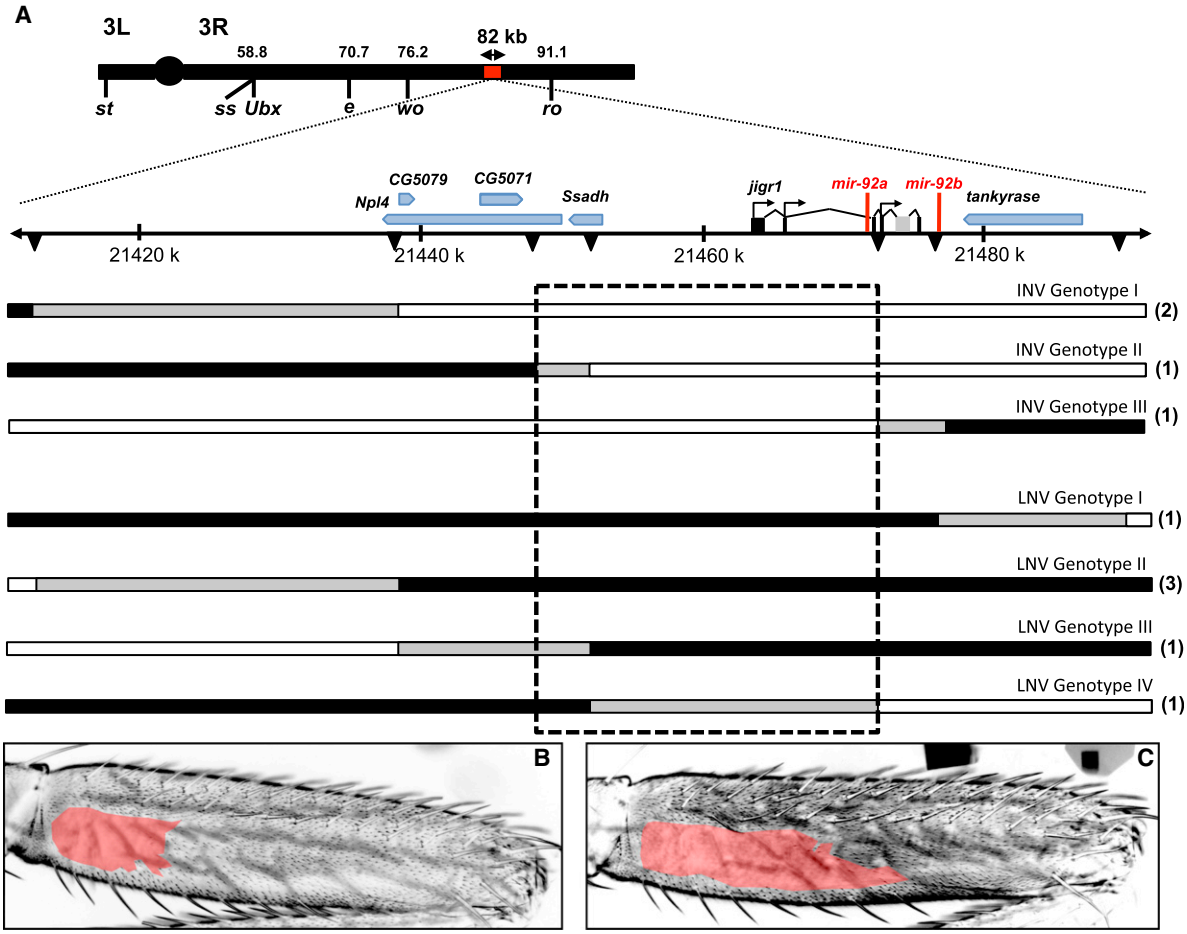

Figure 2. High-Resolution Mapping of the Causative Locus

(A) The topmost black bar represents chromosome 3, with the two arms (3L and 3R) indicated either side of the centromere (circle). The position of *Ubx* and selected QTL markers are shown below the bar, with their positions in cM indicated above. The section of chromosome 3R highlighted by the red bar represents the 82.2 kb evolved region identified by the first mapping experiment (Figure S2C), which is shown expanded below, and between the dotted diagonal lines, with the scale given in kb. The bars below the scale indicate the genotypes of selected recombinants with breakpoints in the 82.2 kb region (note that all flies also carried a nonrecombinant chromosome from strain *e, wo, ro* that is not shown). Positions of molecular markers (Table S2) are indicated by black triangles. The number of individual flies representing each of the selected recombinant genotypes illustrated is given in parentheses to the right. Chromosomal regions from strains *e, wo, ro* (large naked valley parental line) and Oregon-R (small naked valley parental line) are indicated in black and white, respectively. Chromosomal regions in gray indicate DNA where the parental strain identity was not determined. The dashed black box indicates the 25 kb region that underlies naked valley variation. INV and LNV indicate intermediate and large naked valley phenotypes, respectively.

(B and C) Representative examples of T2 posterior femurs from recombinant flies with either an INV (B) or LNV (C).

evolution of *mir-92a* may also contribute to the difference between species, consistent with Stern's evidence for the involvement of another gene [6].

miR-92a Regulates Naked Valley Size through Repression of *shavenoid*

Searches for relevant miR-92a targets showed that the *shavenoid* (*sha*) 3′ UTR contains five highly conserved, canonical seed-match sites (Figures 4A and S4B). *sha* is required for trichome development [18], and its predicted degree of targeting by an individual miRNA exceeds nearly all other genes in *Drosophila* [19]. Therefore, *sha* is well positioned to mediate changes in trichome patterning through altered miR-92a activity. We used luciferase sensor assays to show that the *sha* 3′ UTR is highly and specifically repressed by miR-92a, relative to several other miRNAs that had no effect (Figure 4B). Given that miRNAs often only fine tune their targets by 20% to 30%, even in ectopic tests, the 13-fold regulation we observed indicates a potent regulatory interaction between miR-92a and *sha.*

To test whether *mir-92a* regulates the size of the naked valley via *sha*, we coexpressed *UAS-mir-92a* with a *sha* construct lacking its 3′ UTR [18]. This suppressed the naked valley, and trichomes were found across the posterior T2 femur (Figures 3G and 3H). These results are consistent with the interpretation that miR-92a represses trichomes via downregulation of *sha*. In support of this, we found that *sha* was expressed in a smaller domain in the developing posterior T2 femur of the pupal legs of flies with a LNV compared to those with a SNV (Figures 4F and 4G). Therefore, our in situ results suggest that mRNA degradation is the possible mechanism of repression, but translational blocking could also be involved [9]. Furthermore, it remains possible that miR-92a also regulates other genes involved in trichome formation on the femur.

Although the exact mechanism of *sha* repression via *mir-92a* remains to be resolved, we and others [9, 11] provide

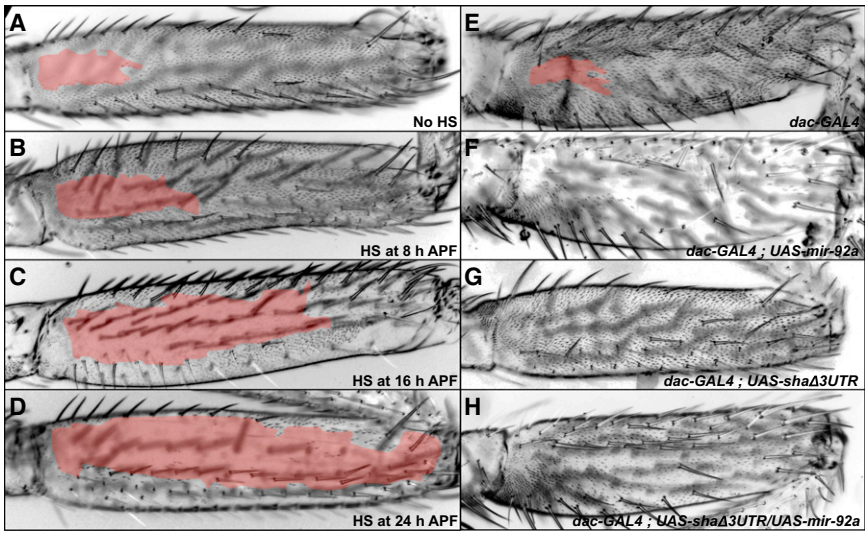

Figure 3. *mir-92a* Represses Trichome Development on the T2 Femur

Uniform expression of *mir-92a* represses trichome formation progressively depending on developmental timing of overexpression induced by heat shock. Tan shading indicates the extent of trichome-free cuticle. See also Figure S3.

(A–D) Posterior of T2 femurs of F1 flies from the cross between *HS-GAL4* and *UAS-mir-92a*.

(A) Posterior T2 femur of a control F1 fly that was not heat shocked.

(B–D) F1 flies heat shocked at 8 hr (B), 16 hr (C), and 24 hr (D) after puparium formation (APF).

(E) Posterior T2 femur of the *dac-GAL4* control line.

(F) *UAS-mir-92a* expression driven by *dac-GAL4* represses trichome formation throughout the posterior femur.

(G) *UAS-shaΔ3UTR* driven by *dac-GAL4* results in the development of ectopic trichomes and removes the naked valley.

(H) Simultaneous overexpression of *UAS-shaΔ3UTR* and *UAS-mir-92a* using *dac-GAL4* leads to rescue of trichome formation and removes the naked valley.

compelling evidence that the *sha* 3′ UTR can be regulated by miR-92a, leading to phenotypic effects consistent with the function of this target gene. Interestingly, *sha* is a known target of the transcription factor Svb, which is thought to act as an input/output integrator to determine where trichomes will develop [10–12] and is a known hotspot for the evolution of larval trichomes [7, 8, 20, 21]. Although presumably *Ubx* acts upstream of *svb* during trichome development, our results show that the modulation of the expression of a downstream gene involved in cytoskeletal organization by a miRNA can also facilitate the evolution of trichome patterns.

Conclusions

We report here the first example of natural variation in the expression of a miRNA causing morphological change. Because the main role of miRNAs is to subtly modulate gene expression levels, variation in the expression and function of such factors appears to be an obvious mechanism to facilitate phenotypic evolution [2, 3]. Although the appearance of new miRNAs and evolutionary changes in the seed sequences of these factors or the 3′ UTRs of their targets have been described [22, 23], the phenotypic consequences of these genetic changes are not known. Therefore, our work represents the first experimental evidence that changes in the *cis*-regulatory sequences of miRNAs contribute to phenotypic evolution.

Experimental Procedures

Morphological Measurements

Dissected T2 legs were mounted in Hoyer's medium and imaged under dark-field or differential interference contrast microscopy using a Leica DM5500 compound microscope and a DFC300 camera. The area of naked valley (μm^2) was measured as the extent of the naked cuticle (without trichomes) starting at the base of the femur (red polygon in Figures 2B and 2C). Femur length (μm) was measured from the proximal end of the femur to the distalmost bristle along the ventral margin.

Fly Lines and Crosses

The stocks *st, ss, e* (Drosophila Genetic Resource Center 101760), Oregon-R, *e, wo, ro* (BL496), and RAL514 [24] were used for mapping experiments.

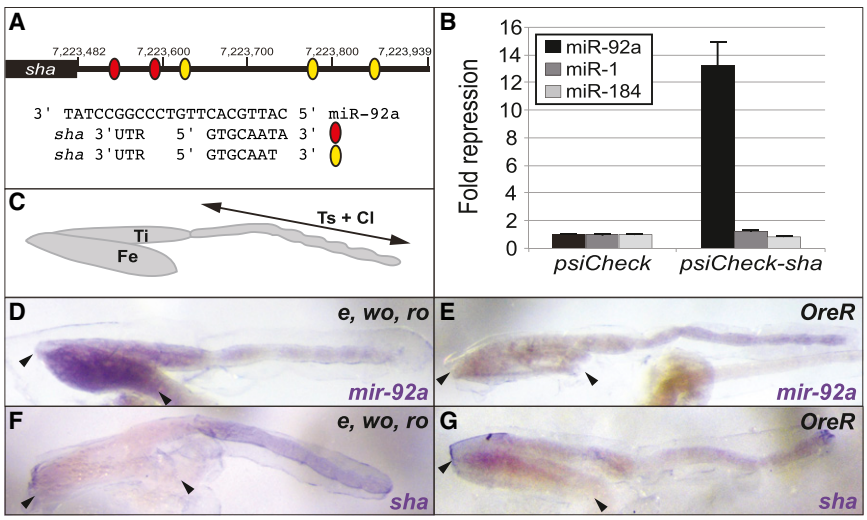

Figure 4. Differential Expression of *mir-92a* Underlies Naked Valley Variation through Repression of *sha*

(A) The *sha* 3′ UTR contains five highly conserved, canonical seed-match sites for miR-92a (see also Figure S4). The black rectangle represents the *sha* coding region and the black line the 3′ UTR. Numbering is with respect to the base-pair position on chromosome 2R. Red and yellow ovals represent predicted seed-match sites for miR-92a consensus sequences shown aligned with the mature miR-92a sequence.

(B) Luciferase sensor assays in S2 cells show that the *sha* 3′ UTR confers >13-fold repression in response to ectopic miR-92a but is unaffected by control miR-1 and miR-184. Error bars show the SD from four independent transfections.

(C) Representation of the T2 pupal leg showing the femur (Fe), tibia (Ti), tarsa (Ts), and claws (Cl).

(D–G) Expression of *pri-mir-92a* (D and E) and *sha* (F and G), in the pupal T2 legs of strains *e, wo, ro* and Oregon-R at 24 hr APF. Arrowheads indicate the femur in each picture.

The stocks *st, ss, e* and Oregon-R were also used to generate reciprocal homozygous recombinant lines for chromosome III (Figure S2B). Transgenic fly stocks used for functional analysis included *w; dac^{GAL4}/Cyo* (referred to as *dac-GAL4* [17]), *w; P(w(+mc)==GAL4-HSP70PB)* (*HS-GAL4*; a gift from Clive Wilson, University of Oxford), *UAS-DsRed-mir-92a* (referred to as *UAS-mir-92a*) [16], *w[*]; P(w(+mC)=UAS-shaGFP)3* (referred to as *UAS-shaΔ3UTR*) [18], *bx-GAL4, ptc-GAL4*, and *sd-GAL4*. All flies and crosses were maintained under standard fly culture conditions. Heat-shock experiments were conducted as described previously [25]. Naked valley sizes were also surveyed from populations of *D. simulans* and *D. melanogaster* [24, 26].

QTL Mapping

Two independent backcross mapping populations were generated for QTL mapping. First, we backcrossed F1 virgin female progeny (from the cross of *st, ss, e* to Oregon-R) to male *st, ss, e* flies. For the second mapping population, we backcrossed F1 virgin female progeny (from the cross of *e, wo, ro* to RAL514) to male *e, wo, ro*. Resultant backcross progeny were phenotyped for naked valley area and T2 femur length and genotyped on chromosome 3 (see Table S2 for genetic markers used). QTL analysis was performed using standard interval mapping with extended Haley-Knott regression [27] with the R package [28]. Additive allelic effects were estimated by fitting linear models for the significant QTL. All analyses were performed with and without femur length as a covariate.

The contribution of chromosomes X, 2, and 4 to variation in naked valley area was assayed by backcrossing male F1 progeny from a cross between Oregon-R and *st, ss, e* to *st, ss, e* females and comparing naked valley area between backcross progeny homozygous or heterozygous for each of these three chromosomes in a homozygous *st, ss, e* chromosome 3 background.

Fine-Scale Mapping

To fine-scale map the causative locus responsible for naked valley variation in the QTL region on 3R, we generated and screened approximately 1,000 recombinants between markers *e* and *msb* and between markers *wo* and *ro* in backcross progeny from crosses between *D. melanogaster* strains *st, ss, e* and Oregon-R and between strains *e, wo, ro* and Oregon-R, respectively. We then measured the naked valley area and femur length of recombinants and mapped the recombination breakpoints using 20 microsatellite, nucleotide, and restriction-site polymorphism markers.

Luciferase Assays

The *shavenoid* 3′ UTR and downstream genomic sequence were cloned into psiCHECK2 (Promega) using a Cold Fusion cloning kit (System Biosciences) and the following primers: Cf_sha3utr_fwd, CCACCTGTTCCTGTAGCG GCCGCATTAGGCTATGCTTAAGTGC; Cf_sha3utr_rev, CCTTCACAAAGA TCCCTCGAGTGAACGCAAAAGTAGCGC. Luciferase assays were carried out as described previously [29]. Briefly, cells were seeded in a 96-well plate at ~1.2 million cells per ml, 100 μl per well. Each well was transfected with 12.5 ng Ub-Gal4 plasmid, 25 ng *UAS-mir* plasmid, and 25 ng pSicheck-derived plasmid using Effectene transfection reagent (QIAGEN). After 3 days, results were read using a Dual-Glo luciferase assay (Promega) and a luminometer (Turner).

In Situ Hybridizations

In situ hybridization was carried out using a standard protocol with DIG-labeled antisense RNA probes. Pupae were fixed at 24 hr APF for 1 hr in 4% formaldehyde after pupal cases were removed. In situ hybridizations were performed with the same concentration of probe for each strain, and the nitro blue tetrazolium/5-bromo-4-chloro-3′-indolyphosphate reaction was stopped at the same time. *pri-mir-92a* and *shavenoid* sequences were cloned into a TOPO PCR4 vector (Invitrogen) using GCAAAATGATGT GAGGCGTA and TCATAAGCAAAATACGAGACAT and AGGAGGATATGGG CATTGTG and TGAACATGGGTGAACTGGAA primer pairs, respectively, following the manufacturer's protocol. M13 forward and reverse primers were used to linearize the DNA. T3 RNA polymerase was used to generate the DIG-labeled riboprobes.

Accession Numbers

Mapping data have been deposited at Dryad (http://datadryad.org/) with the DOI http://dx.doi.org/10.5061/dryad.qd88b.

Supplemental Information

Supplemental Information includes four figures and two tables and can be found with this article online at http://dx.doi.org/10.1016/j.cub.2013.02.018.

Acknowledgments

Work in A.P.M.'s group was funded by the Austrian Science Fund (FWF): M1059-B09, and Oxford Brookes University. Work in E.C.L.'s group was supported by the National Institute of General Medical Sciences of the National Institutes of Health (R01-GM083300). We thank Virginie Orgogozo for fruitful discussions about the project and comments on the manuscript.

Received: December 21, 2012
Revised: February 6, 2013
Accepted: February 7, 2013
Published: February 28, 2013

References

1. Li, J., and Zhang, Z. (2013). miRNA regulatory variation in human evolution. Trends Genet. *29*, 116–124.
2. Niwa, R., and Slack, F.J. (2007). The evolution of animal microRNA function. Curr. Opin. Genet. Dev. *17*, 145–150.
3. Ronshaugen, M., Biemar, F., Piel, J., Levine, M., and Lai, E.C. (2005). The *Drosophila* microRNA *iab-4* causes a dominant homeotic transformation of halteres to wings. Genes Dev. *19*, 2947–2952.
4. Alonso, C.R., and Wilkins, A.S. (2005). The molecular elements that underlie developmental evolution. Nat. Rev. Genet. *6*, 709–715.
5. Davis, G.K., Srinivasan, D.G., Wittkopp, P.J., and Stern, D.L. (2007). The function and regulation of *Ultrabithorax* in the legs of *Drosophila melanogaster*. Dev. Biol. *308*, 621–631.
6. Stern, D.L. (1998). A role of *Ultrabithorax* in morphological differences between *Drosophila* species. Nature *396*, 463–466.
7. Sucena, E., Delon, I., Jones, I., Payre, F., and Stern, D.L. (2003). Regulatory evolution of *shavenbaby/ovo* underlies multiple cases of morphological parallelism. Nature *424*, 935–938.
8. Sucena, E., and Stern, D.L. (2000). Divergence of larval morphology between *Drosophila* sechellia and its sibling species caused by cis-regulatory evolution of *ovo/shaven-baby*. Proc. Natl. Acad. Sci. USA *97*, 4530–4534.
9. Schertel, C., Rutishauser, T., Förstemann, K., and Basler, K. (2012). Functional characterization of *Drosophila* microRNAs by a novel in vivo library. Genetics *192*, 1543–1552.
10. Chanut-Delalande, H., Fernandes, I., Roch, F., Payre, F., and Plaza, S. (2006). Shavenbaby couples patterning to epidermal cell shape control. PLoS Biol. *4*, e290.
11. Delon, I., Chanut-Delalande, H., and Payre, F. (2003). The Ovo/Shavenbaby transcription factor specifies actin remodelling during epidermal differentiation in *Drosophila*. Mech. Dev. *120*, 747–758.
12. Stern, D.L., and Orgogozo, V. (2008). The loci of evolution: how predictable is genetic evolution? Evolution *62*, 2155–2177.
13. DeHoratius, C., and Silver, P.A. (1996). Nuclear transport defects and nuclear envelope alterations are associated with mutation of the *Saccharomyces cerevisiae NPL4* gene. Mol. Biol. Cell *7*, 1835–1855.
14. Rothacker, B., and Ilg, T. (2008). Functional characterization of a *Drosophila melanogaster succinic semialdehyde dehydrogenase* and a non-specific aldehyde dehydrogenase. Insect Biochem. Mol. Biol. *38*, 354–366.
15. Sun, X., Morozova, T., and Sonnenfeld, M. (2006). Glial and neuronal functions of the *Drosophila* homolog of the human SWI/SNF gene ATR-X (DATR-X) and the *jing zinc-finger* gene specify the lateral positioning of longitudinal glia and axons. Genetics *173*, 1397–1415.
16. Bejarano, F., Bortolamiol-Becet, D., Dai, Q., Sun, K., Saj, A., Chou, Y.T., Raleigh, D.R., Kim, K., Ni, J.Q., Duan, H., et al. (2012). A genome-wide transgenic resource for conditional expression of *Drosophila* microRNAs. Development *139*, 2821–2831.
17. Heanue, T.A., Reshef, R., Davis, R.J., Mardon, G., Oliver, G., Tomarev, S., Lassar, A.B., and Tabin, C.J. (1999). Synergistic regulation of vertebrate muscle development by Dach2, Eya2, and Six1, homologs of genes required for *Drosophila* eye formation. Genes Dev. *13*, 3231–3243.

18. Ren, N., He, B., Stone, D., Kirakodu, S., and Adler, P.N. (2006). The *shavenoid* gene of *Drosophila* encodes a novel actin cytoskeleton interacting protein that promotes wing hair morphogenesis. Genetics *172*, 1643–1653.
19. Ruby, J.G., Stark, A., Johnston, W.K., Kellis, M., Bartel, D.P., and Lai, E.C. (2007). Evolution, biogenesis, expression, and target predictions of a substantially expanded set of *Drosophila* microRNAs. Genome Res. *17*, 1850–1864.
20. Frankel, N., Erezyilmaz, D.F., McGregor, A.P., Wang, S., Payre, F., and Stern, D.L. (2011). Morphological evolution caused by many subtle-effect substitutions in regulatory DNA. Nature *474*, 598–603.
21. McGregor, A.P., Orgogozo, V., Delon, I., Zanet, J., Srinivasan, D.G., Payre, F., and Stern, D.L. (2007). Morphological evolution through multiple cis-regulatory mutations at a single gene. Nature *448*, 587–590.
22. Zorc, M., Skok, D.J., Godnic, I., Calin, G.A., Horvat, S., Jiang, Z., Dovc, P., and Kunej, T. (2012). Catalog of microRNA seed polymorphisms in vertebrates. PLoS ONE *7*, e30737.
23. Chen, K., and Rajewsky, N. (2006). Natural selection on human microRNA binding sites inferred from SNP data. Nat. Genet. *38*, 1452–1456.
24. Mackay, T.F., Richards, S., Stone, E.A., Barbadilla, A., Ayroles, J.F., Zhu, D., Casillas, S., Han, Y., Magwire, M.M., Cridland, J.M., et al. (2012). The *Drosophila melanogaster* Genetic Reference Panel. Nature *482*, 173–178.
25. Stern, D.L. (2003). The Hox gene *Ultrabithorax* modulates the shape and size of the third leg of *Drosophila* by influencing diverse mechanisms. Dev. Biol. *256*, 355–366.
26. Pool, J.E., Corbett-Detig, R.B., Sugino, R.P., Stevens, K.A., Cardeno, C.M., Crepeau, M.W., Duchen, P., Emerson, J.J., Saelao, P., Begun, D.J., and Langley, C.H. (2012). Population genomics of Sub-Saharan *Drosophila melanogaster*: African diversity and non-African admixture. PLoS Genet. *8*, e1003080.
27. Haley, C.S., and Knott, S.A. (1992). A simple regression method for mapping quantitative trait loci in line crosses using flanking markers. Heredity (Edinb.) *69*, 315–324.
28. Broman, K.W., Wu, H., Sen, S., and Churchill, G.A. (2003). R/qtl: QTL mapping in experimental crosses. Bioinformatics *19*, 889–890.
29. Okamura, K., Hagen, J.W., Duan, H., Tyler, D.M., and Lai, E.C. (2007). The mirtron pathway generates microRNA-class regulatory RNAs in *Drosophila*. Cell *130*, 89–100.